Supplementary Information for

Property rights and the protection of global marine resources

Gabriel Englander

Corresponding author: Gabriel Englander
Email: englander@berkeley.edu

This PDF file includes:

Table of Contents

Supplementary Methods

1. Data description and availability

The primary AIS dataset in our analysis contains global, daily hours of fishing by gear type and flag state from 2012 to 2016 at a .01 degree resolution[1]. Gear type is the type of fishing activity (e.g. drifting longline fishing). Flag state is the country in which a vessel is registered. Vessels in this data have transponders that send identifying information and their location, speed and course to satellites and terrestrial receivers every 2 to 30 seconds. Convolutional neural networks were applied to this vessel movement data to identify fishing vessels and fishing activity. The creators of this dataset estimate that it captures 50-70% of total fishing effort that occurs more than 100 nautical miles (nm) from shore[1]. This dataset is publicly available at https://globalfishingwatch.force.com/gfw/s/data-download under the heading "Daily Fishing Effort and Vessel Presence at 100th Degree Resolution by Flag State and GearType, 2012-2016."

We used individual fishing vessel characteristics and hours of fishing by individual vessels to construct Supplementary Fig. 6 and Supplementary Table 3. These two datasets are publicly available at the same url as above under the headings "Fishing Vessels Included in Fishing Effort Data" and "Daily Fishing Effort at 10th Degree Resolution by MMSI, 2012-2016", respectively.

Finally, Global Fishing Watch (GFW) provided us with the data used to construct Supplementary Fig. 3. This data contains the last location and date of all instances in which a vessel with a class A AIS transponder stopped transmitting for more than 24 hours. This data can be obtained from GFW upon request.

Daily nighttime locations of individual lit fishing vessels are publicly available at https://data.ngdc.noaa.gov/instruments/remote-sensing/passive/spectrometers-radiometers/imaging/viirs/vbd/v23/global-saa/daily/. This data was created by applying spike detection algorithms to daily nighttime satellite imagery[2]. Vessels in this dataset use bright lights to attract catch. We used data for each day in 2017, as this is the first year in which global data is consistently available.

EEZ access agreements data were provided by the Sea Around Us[3]. This data contains the start and end year of access agreements between countries in which one country pays another country to fish in that country's EEZ. Access agreements can also be multilateral. This data can be requested from the Sea Around Us, or by visiting http://www.seaaroundus.org/data/#/eez, choosing an EEZ, and clicking "Internal Fishing Access Agreements". This data only includes access agreements that began on or before 2014. We added European Union (EU) access

agreements that began after 2014 to this data (the EU is the paying entity). EU access agreements are available at https://ec.europa.eu/fisheries/cfp/international/agreements_en.

EEZ-sea shapefiles are publicly available at http://marineregions.org/download_file.php?name=Intersect_IHO_EEZ_v2_2012.zip[4]. Global, gridded net primary productivity (NPP) data are publicly available at http://www.science.oregonstate.edu/ocean.productivity/standard.product.php[5]. We downloaded 8-day NPP composites from 2012 to 2016 at a .083 degree resolution. Global, gridded ocean depth data at a .0167 degree resolution are publicly available at https://www.ngdc.noaa.gov/mgg/global/relief/ETOPO1/data/bedrock/grid_registered/georeferenced_tiff/ETOPO1_Bed_g_geotiff.zip[6]. Global, gridded sea surface temperature (SST) data are available at https://podaac.jpl.nasa.gov/dataset/MODIS_AQUA_L3_SST_THERMAL_8DAY_4KM_DAYTIME_V2014.0?ids=Measurement:Platform:Sensor:TemporalResolution&values=Ocean%20Temperature:AQUA:MODIS:Weekly. We downloaded 8-day SST composites from 2012 to 2016 at a .041 degree resolution[7]. We downloaded annual, taxon-level catch data for each EEZ-sea region in our analysis from 2012 to 2014 (the most recent year available) from the Sea Around Us using the seaaroundus R package[8, 9]. We obtained life history data for taxa caught in the EEZ-sea regions in our analysis from FishBase and SeaLifeBase using the rfishbase R package[10]. Finally, global, gridded ocean surface currents data are available at ftp://podaac-ftp.jpl.nasa.gov/allData/oscar/preview/L4/oscar_third_deg. We downloaded annual files for 2012 to 2016 that contain surface current velocity at the 5-day, .33 degree resolution[11].

2. Empirical strategy

We use the 200 nautical mile (nm) boundary between EEZs and the high seas as a regression discontinuity to estimate the causal effect of EEZs on fishing effort. In a regression discontinuity, treatment assignment for observation i, D_i, is partially or completely determined by whether a predictor variable, X_i, is above or below a certain cutoff value, c[12]. Let $Y_i(1)$ denote the potential outcome if i is assigned to treatment and $Y_i(0)$ denote the potential outcome if i is assigned to the control group[13]. The assumption in a regression discontinuity design is that $Y_i(1)$ and $Y_i(0)$ are continuous in X_i; they depend on X_i but do not change discontinuously as X_i changes. In other words, if not for the change in treatment assignment at the cutoff value, the outcome variable would change smoothly across the cutoff value. Given this assumption, any discontinuous change in Y_i as X_i crosses the cutoff value is the causal effect of the treatment.

In this paper, after controlling for distance (X_i) to an EEZ-high seas boundary (c), the discontinuous change in fishing effort (Y_i) at the boundary is the causal effect of EEZs (D_i) on fishing effort. We have normalized EEZ-high seas boundaries to be distance 0 ($c = 0$). Observations inside EEZs have positive distance values ($X_i > 0$) and observations on the high

seas have negative distance values ($X_i < 0$). If $X_i > 0$, observations are treated and $D_i = 1$. If $X_i < 0$, $D_i = 0$.

We estimate equations of the following general form via ordinary least squares regression:

$$Y_i = \alpha + \tau D_i + \sum_{k=1}^{K} \beta_k X_i^k + D_i \sum_{k=1}^{K} \gamma_k X_i^k + u_i \quad (1)$$

where Y_i denotes an outcome variable (usually fishing effort), Greek letters denote coefficients, k denotes polynomial order, and u_i denotes the error term. The parameter of interest is τ, the treatment effect of EEZs on the outcome variable. If $\hat{\tau} < 0$, there is a discontinuous decrease in the outcome variable at the boundary (e.g., fishing effort is lower just inside EEZs compared to just outside EEZs). We typically set $K = 3$, which controls for third-order polynomials in distance to the boundary that are allowed to differ for observations inside an EEZ and for observations outside an EEZ.

We provide estimation details for specific figures and tables in the Methods section in the main text of the paper, in Supplementary Methods section 3, and in figure and table captions. Replication code for all figures and tables is available at https://github.com/englander/replication_eez (except for Supplementary Tables 2 and 3, which are summary statistics tables). All analysis was performed in R, except for the calculation of the confidence intervals in Figs. 2 and 4 and Supplementary Figs. 1 and 3-8, which were computed in Stata. Our confidence intervals account for heteroscedasticity and serial correlation[14]. The lag used in calculating each confidence interval was chosen using an optimal lag selection procedure[15].

3. Data processing, analysis, and interpretation of specific figures and tables

Below, we provide additional details on the data processing, analysis, and interpretation of Supplementary Figs. 3-6, Supplementary Fig. 10, and Supplementary Tables 3 and 4.

3.1 Supplementary Fig. 3 information

AIS transponders can be turned off on purpose or can randomly fail to transmit. To account for the latter possibility, we normalized the count of off events for a given vessel type by the hours of vessel presence (i.e. vessel density) for vessels of the same vessel type (see Supplementary Methods section 1 for descriptions of these two datasets). We processed observations of off instances and vessel presence hours into integer bins, summed over all EEZ-sea regions and all days, divided the number of off instances by the number of vessel hours, and multiplied by 10,000 (to get the number of off instances per 10,000 vessel hours).

There is no significant discontinuity in off events at the EEZ-high seas boundary for unauthorized foreign fishing vessels, nor is there a precise trend in off events on either side of the boundary (Supplementary Fig. 3a). Additionally, the frequency of off instances is too low to meaningfully alter estimates of the effect of EEZs on fishing effort. Finally, the nighttime lit vessels dataset provides further evidence that AIS transponder manipulation is not significantly biasing our deterrence effect estimates. Vessels in this dataset use bright lights at night to attract catch. If they are fishing, they appear in the data regardless of whether they are fishing inside an EEZ or fishing on the high seas. The similarity of Fig. 2c (AIS unauthorized foreign fishing) to Fig. 2b (nighttime lit vessel count) therefore provides additional evidence that AIS transponder manipulation is not driving estimated deterrence effects.

There are several reasons why unauthorized foreign vessels would not strategically turn off their AIS transponders in order to avoid detection. The expected benefit of reduced collision risk (from not turning off transponders) could exceed the expected cost of being caught illegally fishing in another nation's EEZ if the probability of being caught is low. Additionally, enforcement agencies may use monitoring systems other than AIS, such as radar.

3.2 Supplementary Fig. 4 and Supplementary Table 4 information

In Supplementary Fig. 4a-e, we test whether our total deterrence effect estimate in Fig. 2c is sensitive to excluding the unauthorized foreign fishing effort observations that are closest to an EEZ-high seas boundary. This test is motivated in part by the concern that our deterrence effect estimates would be too large if enforcement inside EEZs increases unauthorized foreign fishing effort just outside EEZs[16]. This scenario would lead us to overestimate the total deterrence effect of EEZs because our measure of unauthorized foreign fishing effort for the control group (unauthorized foreign fishing effort outside EEZs on the high seas) would be higher than the true counterfactual unauthorized foreign fishing effort if EEZs did not exist. On the other hand, our deterrence effect estimates would be too small if unauthorized foreign vessels reduce high seas fishing effort in advance of EEZ boundaries in order to ensure that they do not accidentally fish inside EEZs (e.g., as drifting longline and purse seine vessels seem to do in Supplementary Fig. 7b,d).

In both of these cases, bias in the total deterrence effect estimate is most likely to occur from unauthorized foreign fishing effort observations that are closest to an EEZ-high seas boundary. By excluding these observations and re-estimating the total deterrence effect, we can get a sense for whether the total deterrence effect estimated reported in Fig. 2c is too large, too small, or robust to these concerns. This type of robustness check is referred to as a "donut regression discontinuity" (donut RD)[17]. We also test in Supplementary Fig. 4 whether our total deterrence effect estimate in Fig. 2c is sensitive to our choice of only analyzing fishing effort that occurs within 50 km of an EEZ-high seas boundary.

Supplementary Fig. 4b-e include unauthorized foreign fishing effort that occurs within 50 km or 100 km of an EEZ-high seas boundary, and exclude observations within 10 km or 25 km of an EEZ-high seas boundary. The range of observations that are included is referred to as the "bandwidth" and the range of observations that are excluded is referred to as the "donut hole". For example, Supplementary Fig. 4c uses unauthorized foreign fishing effort within 100 km of an EEZ-high seas boundary (bandwidth is 100 km), but drops observations within 10 km of an EEZ-high seas boundary (donut hole is 10 km). We control for a linear trend in distance to an EEZ-high seas boundary instead of a third-order polynomial because donut RDs require extrapolating through the donut hole to the discontinuity cutoff value (see Supplementary Fig. 4b-e). Supplementary Fig. 4a replicates Fig. 2c with a linear trend. When assessing how our various donut RD specifications change the total deterrence effect estimate, we always compare our donut RD estimates to the estimate in Supplementary Fig. 4a.

Every combination of different bandwidths and donut holes yields deterrence effect estimates that are .3 to 2 percentage points larger than our baseline estimate in Supplementary Fig. 4a (see Supplementary Table 4 for numeric estimates corresponding to Supplementary Fig. 4a-e). This exercise suggests that the total deterrence effect estimate displayed in Fig. 2c is not biased by the potential spillover concerns described above.

Supplementary Fig. 4f displays an additional test for whether enforcement inside EEZs causes spillovers of unauthorized foreign fishing into control regions (high seas regions within 50 km of an EEZ). As discussed above, this type of spillover would make our deterrence effect estimates upward biased. The intuition for the test in Supplementary Fig. 4f is that EEZs whose control regions have a greater degree of overlap with the control regions of other EEZs should have larger deterrence effects, all else equal, if this type of spillover is causing upward bias in our deterrence effect estimates. The reason that EEZs with more control region overlap would have greater deterrence effect estimates is that their control regions would be receiving enforcement-induced spillovers from other EEZs in addition to own-EEZ spillovers. For example, the control region corresponding to Iceland's EEZ in the Norwegian Sea would be receiving spillovers from other EEZs that surround the high seas of the Norwegian Sea (Norway, Denmark, Greenland, and the Faroe Islands) in addition to receiving own-spillovers (from enforcement of Iceland's EEZ).

For each EEZ-sea region, we calculate the fraction of its control region that is overlapping with the control regions of other EEZ-sea regions (minimum value = 0, 25^{th} percentile = .07, median = .16, 75^{th} percentile = .40, maximum = 2.17). An EEZ-sea region's overlap fraction exceeds 1 when the area of overlap with every other control region is larger than the area of the EEZ-sea region's control region. Following the same procedure used to create Fig. 4a, we first grouped the 178 EEZ-sea regions with more than zero AIS fishing hours into 20 quantiles according to their control region's overlap fraction. Then we estimated equation (2) (in

Methods section in the main text) via ordinary least squares regression, obtaining a separate deterrence effect for each quantile group. Recall that the dependent variable in this regression is hours of unauthorized foreign fishing per thousand km^2 for a given EEZ-sea region and integer bin.

In Supplementary Fig. 4f, overlap fraction groups farther to the right on the x-axis contain EEZ-sea regions with larger overlap fractions. If spillovers cause upward bias in our estimates, deterrence effects should be increasing to the right along the x-axis. In fact, deterrence effects are slightly decreasing in overlap fraction, though the trend is not statistically significant (p-value from regressing overlap fraction group deterrence effect on a constant and a linear trend in overlap fraction group number is .34; N=20). Supplementary Fig. 4f therefore provides further evidence that our deterrence effect estimates are not biased by potential spillovers.

3.3 Supplementary Fig. 5 information

Some countries, such as China and Taiwan, do not make their EEZ access agreements publicly available. Vessels from these countries are therefore always classified as unauthorized foreign when they are fishing closest to any EEZ other than their home country. As a consequence, we may be underestimating deterrence effects by misclassifying vessels that are actually authorized foreign. This misclassification would lead to underestimated deterrence effects because unlike unauthorized foreign vessels, authorized foreign vessels are more likely to fish just inside EEZs (Fig. 2d). Supplementary Fig. 5a plots unauthorized foreign fishing by vessels from (flagged to) countries with at least one public access agreement. Supplementary Fig. 5b plots unauthorized foreign fishing by vessels from countries with no public access agreements (e.g. Chinese vessels). The deterrence effect in both figures is about 80%, suggesting that incomplete access agreements data is not significantly affecting our results.

3.4 Supplementary Fig. 6 and Supplementary Table 3 information

GFW provides two global, daily fishing hours datasets: .01 degree resolution data at the flag state-gear type level (the primary dataset used in this paper) and .1 degree resolution data at the individual vessel level. The latter data contains vessels' MMSI, a unique identifier, which we joined to a third GFW dataset containing estimated vessel gear type, gross tonnage, length, and engine power[1]. We matched .01 degree resolution fishing observations to .1 degree resolution observations in order to add vessel characteristics to the .01 degree resolution dataset. We uniquely matched 79.4% of .01 degree resolution fishing hours observations to .1 degree resolution fishing hours observations. We used the variables these two datasets have in common to match observations across them: the location, date, gear type, flag state, and quantity of fishing hours. We calculated fishing hours-weighted average vessel characteristics for the .01 degree resolution observations that matched to multiple .1 degree resolution observations. We use the dataset created at this stage to create Supplementary Table 3.

For Supplementary Fig. 6, we then calculated fishing hours-weighted median gross tonnage, length, and engine power for each vessel type and for each gear type. We used these median values to classify fishing hours observations as belonging to above or below median vessels. We then summed fishing hours observations over all EEZ-sea regions and over all days, and divided by the surface area in each integer bin in millions of km^2.

Supplementary Fig. 6 shows that larger vessels (in terms of gross tonnage) have larger discontinuities at the boundary, suggesting they are more able to choose their fishing locations strategically (e.g. because of superior technology). Larger unauthorized foreign vessels are more able to "fish the line" just outside EEZs on the high seas, and larger authorized foreign and domestic vessels are more able to avoid competing with unauthorized foreign vessels on the high seas by fishing just inside EEZs. Larger unauthorized foreign vessels also account for a larger proportion of unauthorized fishing inside EEZs. These results are unchanged when vessel length or engine power are used to divide vessels into above and below median size (available upon request).

3.5 Supplementary Fig. 10 information

EEZ-sea regions with fish stocks that move more frequently across their high seas boundaries could have larger deterrence effects if unauthorized foreign vessels are more likely to fish just outside these EEZs (e.g., in order to catch fish as they swim from the EEZ into the high seas). We use two measures of fish mobility to test this hypothesis. First, we compute the fraction of an EEZ-sea region's catch that is from oceanodromous species. Oceanodromous fish are migratory fish that spend their entire life in the ocean. Second, we compute the average ocean surface current direction at the EEZ-high seas boundary for each EEZ-sea region. EEZ-sea regions in which the current typically flows out of the EEZ toward the high seas might have more unauthorized foreign vessels fishing just outside the EEZ on the high seas (and thus have larger deterrence effects). After computing these two values for each EEZ-sea region, we follow the same procedure used to generate Fig. 4a in order to non-parametrically estimate a relationship between deterrence effects and these two measures of fish mobility.

We computed the fraction of an EEZ-sea region's catch that is from oceanodromous species as follows. First, we downloaded annual, taxon-level catch data for each EEZ-sea region in our analysis from 2012 to 2014 (the most recent year available) from the Sea Around Us using the seaaroundus R package[8, 9]. We dropped observations that contained "Miscellaneous" or "fishes not identified" in the "taxon_scientific_name" column (e.g., "Miscellaneous marine crustaceans" and "Marine fishes not identified"). For each EEZ-sea region-taxon pair, we queried FishBase and SeaLifeBase for the taxon's migration patterns using the rfishbase package[10]. Species migration patterns are recorded in the "AnaCat" variable in the Species Table in FishBase and SeaLifeBase and can take the following values: anadromous, catadromous, amphidromous, potamodromous, limnodromous, oceanodromous, non-migratory, and missing.

In cases without an initial match between a Sea Around Us taxon name and scientific name(s) in FishBase or SeaLifeBase, we iteratively queried FishBase and SeaLifeBase at higher taxonomic classifications until we found a match. For example, if the Sea Around Us taxon name was "Gadiformes" (an order), we obtained the AnaCat variable of all species in the Gadiformes order. In all cases, we filtered FishBase/SeaLifeBase observations to those in the same FAO region as the EEZ-sea region and dropped FishBase/SeaLifeBase observations that were missing an AnaCat value. If we obtained migration patterns for the same species from both FishBase and SeaLifeBase, we used the migration pattern value from FishBase. We computed the fraction of species that are oceanodromous for EEZ-sea region-taxon pairs that had multiple FishBase/SeaLifeBase matches. For example, we calculated that 71% of Gadiformes species that are likely present in the Irish part of the North Atlantic Ocean are oceanodromous.

After determining whether each EEZ-sea region-taxon pair is oceanodromous (or the fraction that is oceanodromous), we computed the weighted fraction of an EEZ-sea region's catch that is oceanodromous, using the tons caught of each taxon in the EEZ-sea region between 2012 and 2014 as weights. We thus obtained a value between 0 and 1 for each EEZ-sea region (minimum value = 0, 25th percentile = .70, median = .92, 75th percentile = .99, maximum = 1). We were unable to compute this value for the South Georgian part of the Southern Ocean because all of its Sea Around Us taxa were "Miscellaneous", "fishes not identified", or had missing AnaCat values in FishBase and SeaLifeBase. However, we were able to compute this value for all other EEZ-sea regions in our analysis. We also computed the fraction of an EEZ-sea region's catch that are not non-migratory, but found that this variable had less variation across EEZ-sea regions (minimum value = .29, 25th percentile = .72, median = .99, 75th percentile = .998, maximum = 1).

We computed average ocean surface current direction at each EEZ-sea region's high seas boundary as follows. We downloaded surface current velocity data from 2012 to 2016 from NASA's Earth Space Research group[11]. The data contain surface current velocity at the 5-day, .33 degree resolution. For each observation intersecting a given EEZ-sea region's high seas boundary, we calculated whether the current was moving away from the centroid of the EEZ-sea region. We recorded a value of 1 if it was, and recorded a value of 0 otherwise. We then calculated the average current direction over all grid cells and all 5-day periods for each EEZ-sea region. We thus obtained a value between 0 and 1 for each EEZ-sea region (minimum value = .11, 25th percentile = .45, median = .52, 75th percentile = .57, maximum = .85). A value of 0 would indicate that the current is always flowing into the EEZ-sea region at the EEZ-sea region's high seas boundary, and a value of 1 would indicate that the current is always flowing out of the EEZ-sea region at the EEZ-sea region's high seas boundary.

We created Supplementary Fig. 10a,b using the same procedure we implemented to create Fig. 4a (see Methods section in main text). We first grouped the EEZ-sea regions with

more than zero AIS fishing hours into 20 quantiles according to their fraction of catch from oceanodromous species (Supplementary Fig. 10a) and average surface current direction (Supplementary Fig. 10b). There are 8 or 9 EEZ-sea regions in each quantile group. Then we estimated equation (2) (in Methods section in main text) via ordinary least squares regression, obtaining a separate deterrence effect for each quantile group.

In both parts of Supplementary Fig. 10, quantile groups farther to the right on the x-axis are expected to contain EEZ-sea regions with fish stocks that move more frequently from EEZs into the high seas. If unauthorized foreign vessels are more likely to locate themselves just outside these EEZs in order to catch fish as they swim from these EEZs into the high seas, then deterrence effects should be increasing to the right along the x-axis. However, neither Supplementary Fig. 10a nor Supplementary Fig. 10b exhibit a trend in deterrence effects. p-values from regressing quantile group-specific deterrence effects on a constant and a linear trend in quantile group number are .21 and .89, respectively (N=20). By contrast, deterrence effects clearly increase in average NPP. The p-value from regressing the NPP quantile group-specific deterrence effect estimates in Fig. 4a on a constant and a linear trend in quantile group number is .01 (N = 20). The two proxies for fish mobility we have examined in this section seem to be less important for understanding deterrence effect heterogeneity than NPP, a proxy for fishery value (see main text).

4. The historical origins of 200 nautical mile-wide EEZs

In 1947, Chile became the first nation to declare a 200 nm exclusive zone. The lawyer in charge of finding a legal precedent for this unilateral declaration chose 200 nm to match his imprecise map of a neutrality zone around Chile that was declared by the United States in 1939. The width of the neutrality zone was actually 300 nm[18]. In the ensuing decades, other countries followed Chile's precedent, and the right of coastal nations to a 200 nm EEZ was finally codified at the third UN Conference on the Law of the Sea between 1973 and 1982[19]. Nations with fewer than 400 nm of ocean separating them typically divide the available ocean area equally. We only use EEZ boundaries that are 200 nm from shore and border the high seas in our analysis.

This history supports the assumption that is necessary for our regression discontinuity design to be valid (Supplementary Methods section 2), because it suggests that it is very unlikely that unobservable variables that affect fishing change discontinuously at EEZ-high seas boundaries. The 200 nm maximum width for EEZs was not chosen because fishing opportunities change discontinuously at this distance from shore, so it is very likely that discontinuous changes in fishing at EEZ-high seas boundaries are due to the discontinuous change in institutions at these boundaries (EEZs on one side and not the other).

5. Theoretical models predicting that more valuable EEZs have larger deterrence effects and more enforcement effort

We develop two theoretical models in this section to show that (Claim 1) EEZs that are more valuable near their high seas boundaries have larger deterrence effects and (Claim 2) countries with EEZs that are more valuable near their high seas boundaries find it in their interest to exert more enforcement effort. Section 5.1 demonstrates that our empirical result in Fig. 4 can be supported by economic theory. Section 5.2 shows that our explanation for the empirical result in Fig. 4, that countries are incentivized to exert more enforcement effort if their EEZs are more valuable, can also be supported by economic theory.

5.1 Claim 1: Deterrence effects are increasing in EEZ value

Suppose a representative unauthorized foreign fishing vessel maximizes profit (π) by choosing fishing effort just inside a given EEZ (i), fishing effort just outside the EEZ (o), and fishing effort everywhere else (e). We develop a static model for simplicity and because our empirical analysis is a spatial cross-section. Revenue from fishing just inside or just outside the EEZ is $R(i, o;\ v)$, where v is a fixed (exogenous) parameter representing the "value" or quality of the fishery near the EEZ boundary. Revenue from fishing effort everywhere else is $M(e)$. Suppose the cost of a unit of fishing effort is c. Then fishing effort costs are linear in total fishing effort and equal $(i\ +\ o\ +\ e)c$. Finally, fishing opportunities are identical just inside and just outside the EEZ except that the vessel incurs an additional cost $\sigma(i)$ from fishing just inside the EEZ that reflects the probability of being punished for illegal fishing and the magnitude of punishment (e.g. fine level) if punishment occurs. We refer to $\sigma(i)$ as the vessel's expected punishment cost.

Let subscripts denote partial derivatives with respect to a function's argument and let $(\cdot)$ indicate that a function's arguments have been suppressed. We make the following assumptions. First, the vessel's expected punishment cost from illegally fishing just inside the EEZ is increasing and convex ($\sigma_i(i) > 0$ and $\sigma_{ii}(i) > 0$). Second, both revenue functions are increasing and concave in fishing effort ($R_i(\cdot), R_o(\cdot), M_e(e) > 0$, and $R_{ii}(\cdot), R_{oo}(\cdot), M_{ee}(e) < 0$). Third, the marginal increase in revenue from increasing fishing effort just inside or just outside the EEZ is increasing in the value of the fishery near the EEZ boundary ($R_{iv}(\cdot), R_{ov}(\cdot) > 0$). Because fishing revenue opportunities are identical just inside and just outside the EEZ, we assume that these terms are equal ($R_{iv}(\cdot) = R_{ov}(\cdot)$), and also assume that $R_{ii}(\cdot) = R_{oo}(\cdot)$.

The vessel's decision problem is:

$$\max_{i,o,e} \pi = R(i, o; v) + M(e) - (i + o + e)c - \sigma(i)$$

The vessel's first-order conditions (FOCs) with respect to i, o, and e are:

FOC i: $R_i(\cdot) - c - \sigma_i(i) = 0$

FOC o: $R_o(\cdot) - c = 0$

FOC e: $M_e(e) - c = 0$

The deterrence effect, τ, for a given EEZ is total unauthorized foreign fishing effort just inside the EEZ minus total unauthorized foreign fishing effort just outside the EEZ. Let * indicate the optimized value of a choice parameter (e.g. i^*). The difference in the representative unauthorized foreign vessel's fishing effort just inside the EEZ and just outside the EEZ is $i^* - o^*$ and is given by the above three first-order conditions. In the context of this model, since unauthorized foreign vessels are identical, $\tau = (i^* - o^*)N$, where N is the number of unauthorized foreign fishing vessels. EEZs that deter unauthorized foreign fishing have $\tau < 0$. Claim 1 is that deterrence effects are increasing (becoming larger negative numbers) as the value of the fishery near the EEZ boundary increases. Mathematically, this claim is $\frac{d\tau}{dv} = \left(\frac{di^*}{dv} - \frac{do^*}{dv}\right) N < 0$. We show this claim by totally differentiating the three first-order conditions with respect to i, o, e, and v, and applying Cramer's Rule to derive $\frac{di^*}{dv}$ and $\frac{do^*}{dv}$.

$$\begin{bmatrix} R_{ii}(\cdot) - \sigma_{ii}(i) & R_{io}(\cdot) & 0 \\ R_{oi}(\cdot) & R_{oo}(\cdot) & 0 \\ 0 & 0 & M_{ee}(e) \end{bmatrix} \begin{bmatrix} di \\ do \\ de \end{bmatrix} = \begin{bmatrix} -R_{iv}(\cdot) \\ -R_{ov}(\cdot) \\ 0 \end{bmatrix} dv$$

Applying Cramer's Rule to the above system of equations gives $\frac{di^*}{dv} > 0$ and $\frac{do^*}{dv} > 0$ as long as $R_{oo}(\cdot) < R_{io}(\cdot)$ (equivalently, $R_{ii}(\cdot) < R_{oi}(\cdot)$). This condition means that increasing fishing effort in the same location causes a larger decrease in marginal revenue than increasing fishing effort in the adjacent location.

Though fishing effort just inside and just outside the EEZ both increase in the value of this fishery v, fishing effort just inside the EEZ increases by a relatively smaller amount. Intuitively, the potential revenue from fishing just inside and just outside the EEZ increases by the same amount, but less fishing effort is allocated to just inside the EEZ because of the risk of being punished for illegally fishing inside the EEZ. To see this mathematically, let A denote the above 3x3 matrix (the left-hand side matrix) and let $det(A)$ denote the determinant of A. Then $\frac{d\tau}{dv} = \left(\frac{di^*}{dv} - \frac{do^*}{dv}\right) N = \frac{-R_{iv}(\cdot) M_{ee}(e) \sigma_{ii}(i)}{det(A)} N$. Since $R_{iv}(\cdot) > 0, M_{ee}(e) < 0$, and $\sigma_{ii}(\cdot) > 0$, the numerator of $\frac{d\tau}{dv}$ is positive. Since $det(A)$ is negative by the second-order condition for a

maximum, $\frac{d\tau}{dv} < 0$. Deterrence effects are increasingly large (more negative) as the value of the fishery near the EEZ boundary increases.

5.2 Claim 2: Enforcement effort is increasing in EEZ value

Now consider a country choosing enforcement effort z to minimize the quantity of unauthorized foreign fishing effort inside its EEZ and the cost of enforcement effort, $c(z)$. Let $I(z; v)$ denote total unauthorized foreign fishing effort inside the country's EEZ, where v represents the exogenous component of the fishery's value. Other variables may affect unauthorized foreign fishing effort inside the EEZ, such as fishing opportunities in other locations, but it is not necessary to model them explicitly in order to support Claim 2. Note that for the purposes of supporting Claim 2, the country minimizing unauthorized foreign fishing effort inside its EEZ is equivalent to the country minimizing unauthorized foreign catch inside its EEZ (since catch is a function of fishing effort). As before, we have developed a static model for simplicity and because our empirical analysis is a spatial cross-section.

We assume that unauthorized foreign fishing effort inside the EEZ is decreasing in enforcement effort ($I_z(z; v) < 0$). We also assume that the marginal decrease in unauthorized foreign fishing effort from additional enforcement effort is increasing (becoming less negative) as fishery value increases ($I_{zv}(z; v) > 0$). Intuitively, this assumption means that additional enforcement effort "buys" less deterrence when the fishery is more valuable because unauthorized foreign vessels are more willing to risk punishment in order to access a more valuable fishery.

The country solves:

$$\max_z -I(z; v) - c(z)$$

Note that maximizing the negative of $I(z; v)$ and $c(z)$ is equivalent to minimizing $I(z; v) + c(z)$. The first-order condition with respect to z is:

$$-I_z(z; v) - c_z(z) = 0$$

Totally differentiating the first-order condition with respect to z and v and then re-arranging terms gives $\frac{dz}{dv} = \frac{-I_{zv}(z;v)}{I_{zz}(z;v)+c_{zz}(z)}$. Since $I_{zv}(z; v) > 0$, the numerator is negative. The denominator is also negative by the second-order condition for a maximum. Therefore, enforcement effort is increasing in EEZ fishery value ($\frac{dz}{dv} > 0$). Intuitively, if fishery value increases, $I(z; v)$ increases, all else equal. But the cost of enforcement effort for the country $c(z)$ has not changed. Enforcement effort increases with fishery value because the marginal benefit of

an additional unit of enforcement effort (in terms of a reduction in unauthorized foreign fishing inside the EEZ) increases more than the marginal cost of an additional unit of enforcement effort.

Supplementary Figures

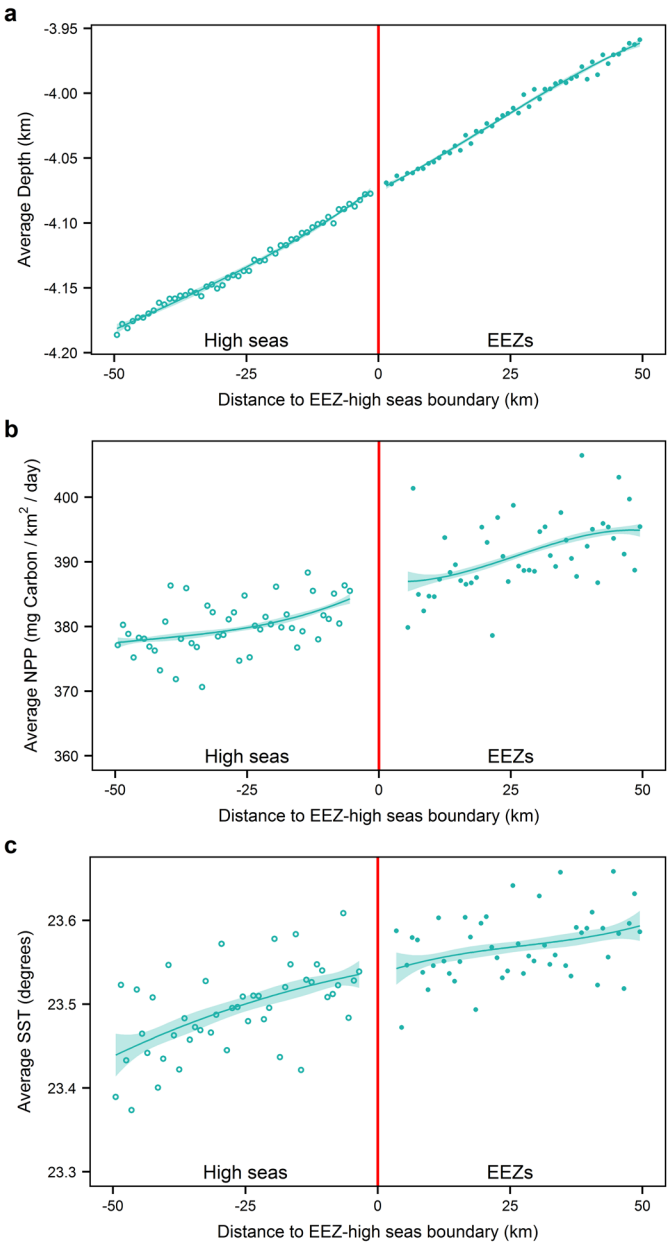

Supplementary Fig. 1. No other discontinuities at EEZ-high seas boundaries. Average (**a**) ocean depth, (**b**) net primary productivity (NPP), and (**c**) sea surface temperature (SST) with respect to an EEZ-high seas boundary. Grid cells are assigned to the minimum integer bin (over all EEZ-sea regions) that their cell center intersects (see Methods in main text). Weighted average values over all EEZ-sea regions are calculated using grid cell areas (all variables) and the number of days each composite comprises (NPP and SST only) as weights. NPP and SST averages are calculated using data between 2012 and 2016. Points are data. Lines are ordinary least squares third-order polynomial fits in distance to the boundary. 95% confidence intervals (shaded) are estimated using standard errors that account for heteroscedasticity and serial correlation[14].

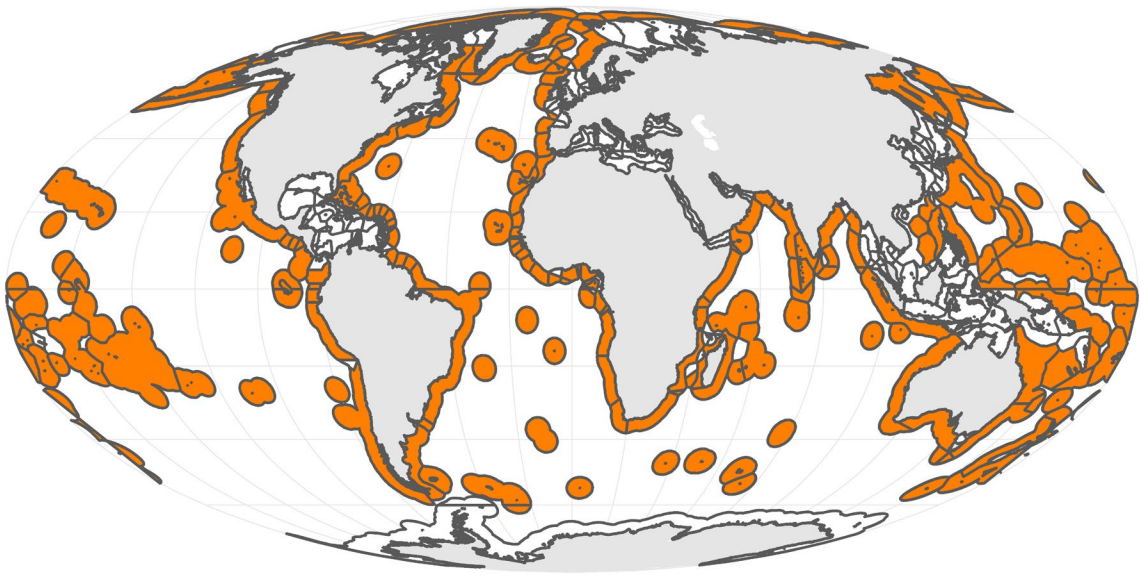

Supplementary Fig. 2. EEZ-sea regions in analysis. EEZ-sea regions that are 200 nm wide and border the high seas are filled orange. Note that we have filled the entire area of these EEZ-sea regions for visibility, but only analyze fishing effort that occurs within 50 km of an EEZ-high seas boundary. All other EEZ-sea regions are unfilled. Antarctica is excluded from the analysis because its resources do not belong to a single nation.

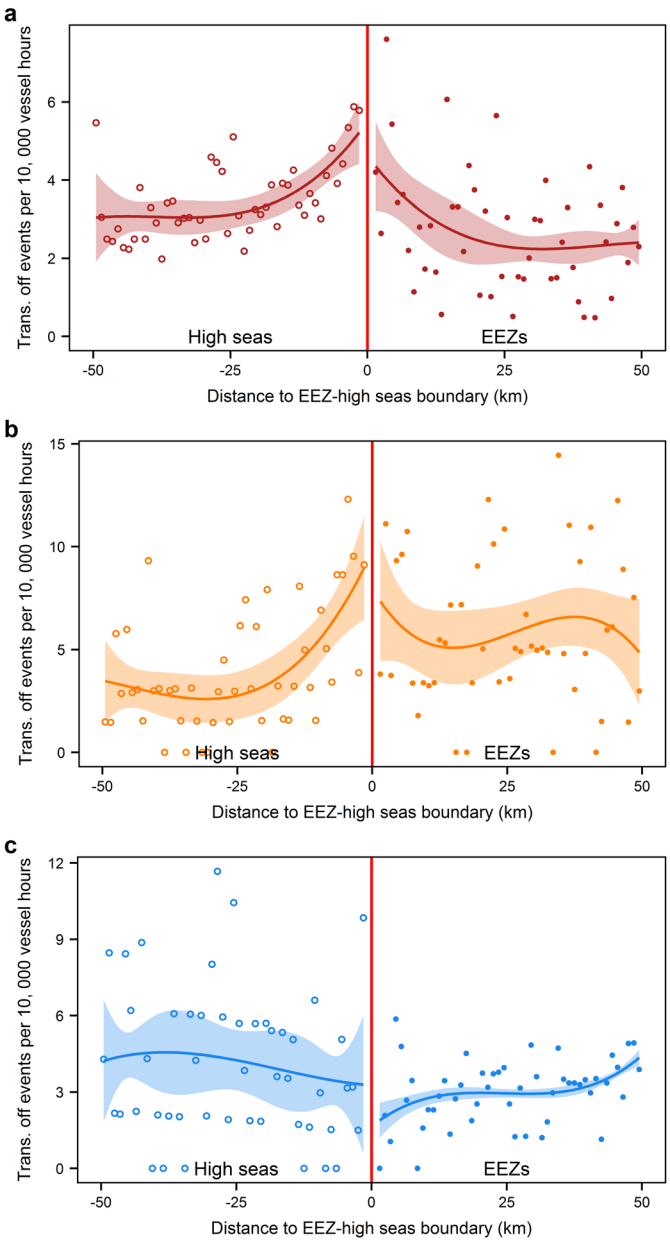

Supplementary Fig. 3. AIS transponder off events by distance to an EEZ-high seas boundary. Off events per 10,000 hours of AIS vessel presence between 2012 and 2016 for (**a**) unauthorized foreign fishing vessels, (**b**) authorized foreign fishing vessels, and (**c**) domestic fishing vessels. See Supplementary Methods section 3.1 for a discussion of this figure. Points are data. Lines are ordinary least squares third-order polynomial fits in distance to the boundary. 95% confidence intervals (shaded) are estimated using standard errors that account for heteroscedasticity and serial correlation[14].

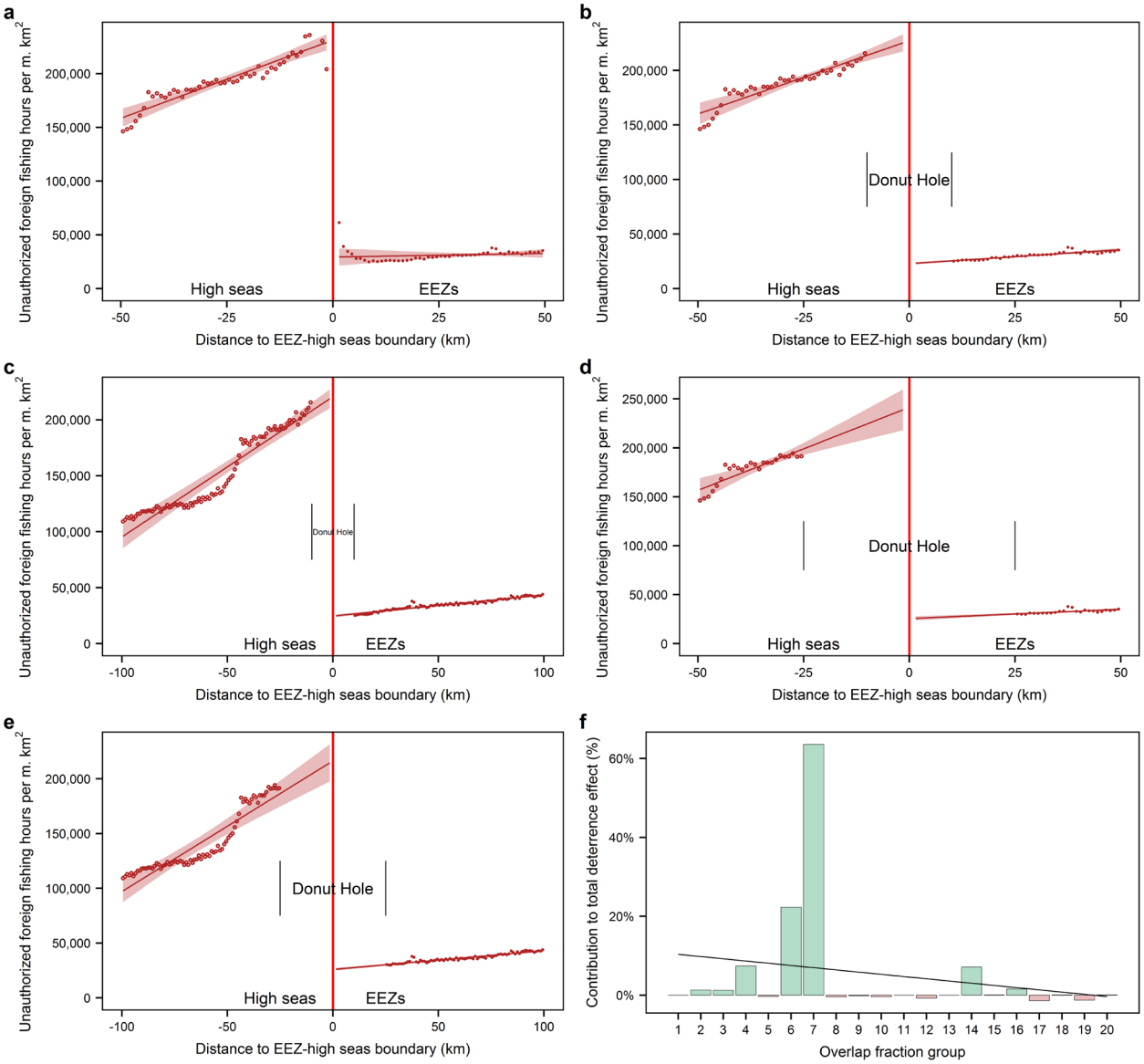

Supplementary Fig. 4. Robustness of deterrence effect estimates to potential spillovers. Deterrence effect estimate using (**a**) all observations within 50 km of an EEZ-high seas boundary, (**b**) observations between 10 and 50 km from a boundary, (**c**) observations between 10 and 100 km from a boundary, (**d**) observations between 25 and 50 km from a boundary, and (**e**) observations between 25 and 100 km from a boundary. See Supplementary Table 4 for numerical point estimates corresponding to these figures. Points are data. We control for a linear trend in distance to the boundary instead of a third-order polynomial because higher-order polynomials are unsuitable for extrapolating to the boundary, as is required in a donut RD. 95% confidence intervals (shaded) are estimated using standard errors that account for heteroscedasticity and serial correlation[14]. (**f**) Contribution of each overlap fraction group to the total deterrence effect. We estimate a deterrence effect for each overlap fraction group, and divide each group's effect by the sum of all groups' deterrence effects. Overlap fraction groups that contribute a positive percentage (green) deter unauthorized foreign fishing. The black line is a linear trend. See Supplementary Methods section 3.2 for a discussion of this figure.

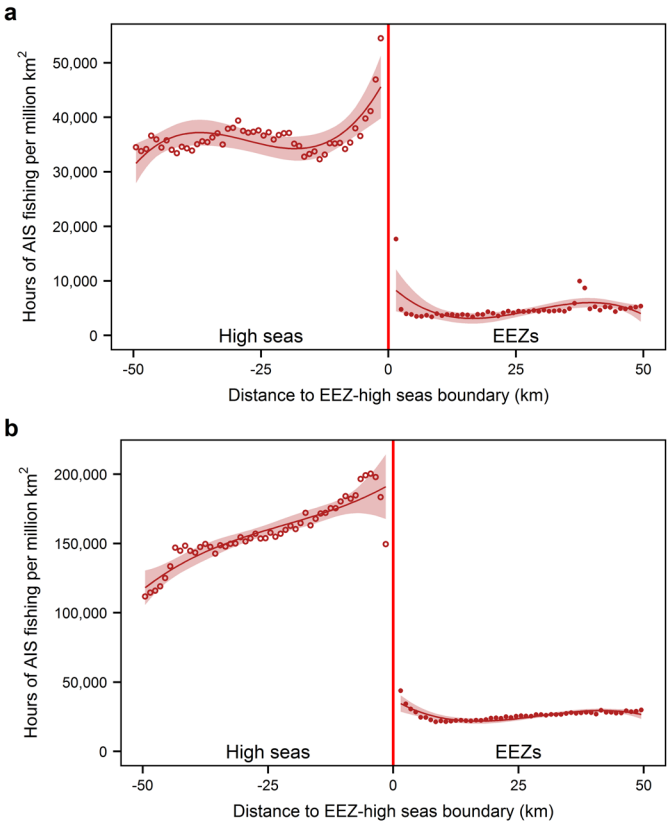

Supplementary Fig. 5. Unauthorized foreign fishing by availability of EEZ access agreements. Unauthorized foreign fishing by vessels from countries that (**a**) make their access agreements publicly available and (**b**) do not publish their access agreements. See Supplementary Methods section 3.3 for a discussion of this figure. Points are data. Lines are ordinary least squares third-order polynomial fits in distance to the boundary. 95% confidence intervals (shaded) are estimated using standard errors that account for heteroscedasticity and serial correlation[14].

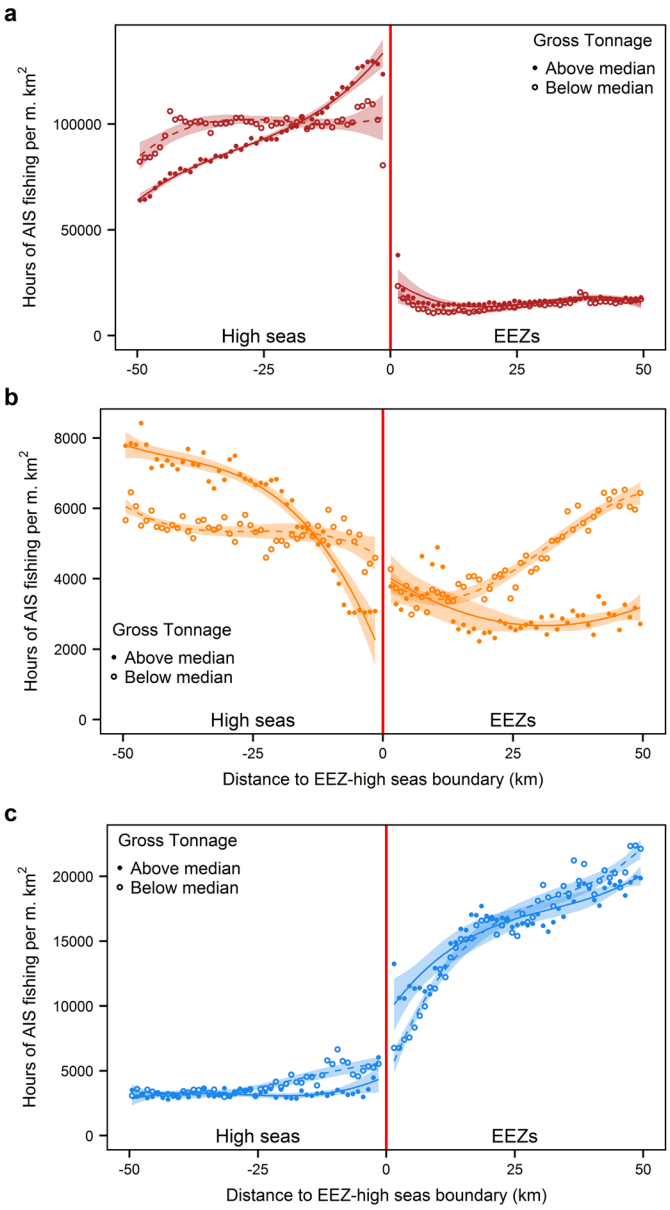

Supplementary Fig. 6. Larger fishing vessels have larger discontinuities. Fishing by above and below median gross tonnage (**a**) unauthorized foreign vessels, (**b**) authorized foreign vessels, and (**c**) domestic fishing vessels. See Supplementary Methods section 3.4 for a discussion of this figure. Points are data. Lines are ordinary least squares third-order polynomial fits in distance to the boundary. 95% confidence intervals (shaded) are estimated using standard errors that account for heteroscedasticity and serial correlation[14].

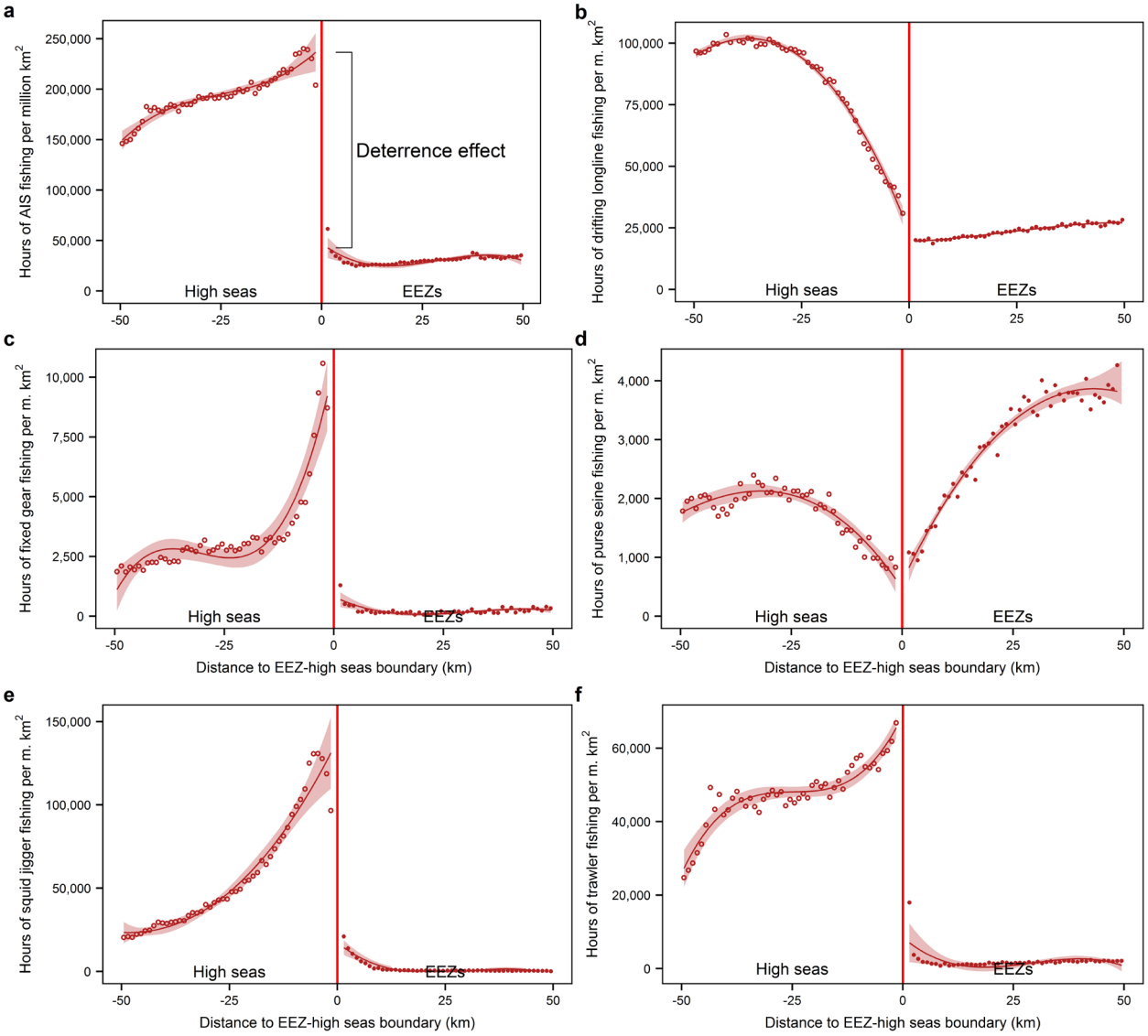

Supplementary Fig. 7. Deterrence effect by gear type. **a**, Hours of fishing by unauthorized foreign vessels for all gear types (equivalent to Fig. 2c; reproduced here for reference). Hours of unauthorized foreign (**b**) drifting longline fishing, (**c**) fixed gear fishing, (**d**) purse seine fishing, (**e**) squid jigger fishing, and (**f**) trawler fishing. Points are data. Lines are ordinary least squares third-order polynomial fits in distance to the boundary. 95% confidence intervals (shaded) are estimated using standard errors that account for heteroscedasticity and serial correlation[14].

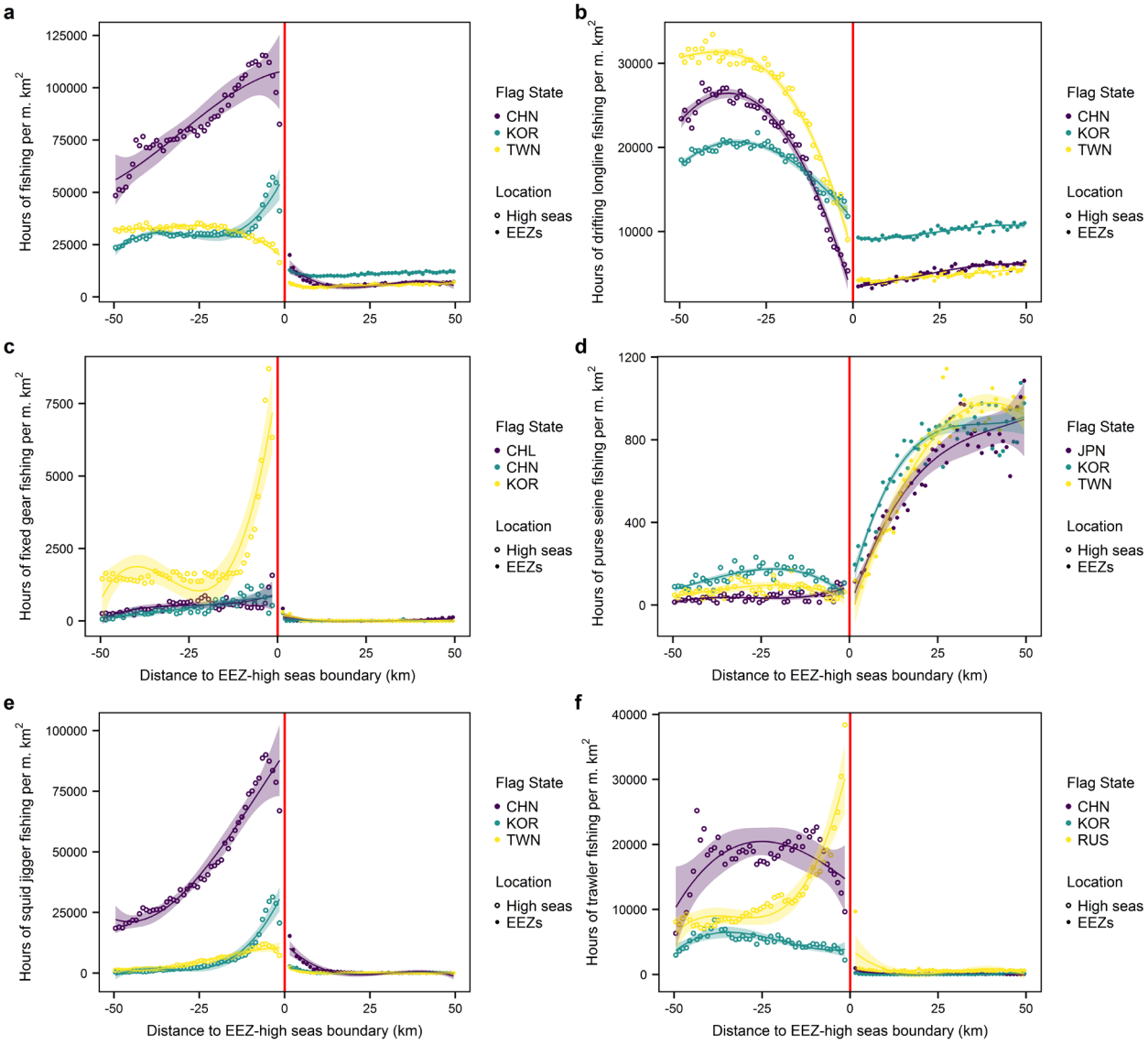

Supplementary Fig. 8. Unauthorized foreign fishing for the top three flag states (fishing countries) in each gear type. (**a**) All gear types, (**b**) drifting longline fishing, (**c**) fixed gear fishing, (**d**) purse seine fishing, (**e**) squid jigger fishing, and (**f**) trawler fishing. We calculated the top three flag states for each gear type in terms of total hours of unauthorized foreign fishing within 50 km of any EEZ-sea region in our analysis between 2012 and 2016. Points are data. Lines are ordinary least squares third-order polynomial fits in distance to the boundary. 95% confidence intervals (shaded) are estimated using standard errors that account for heteroscedasticity and serial correlation[14].

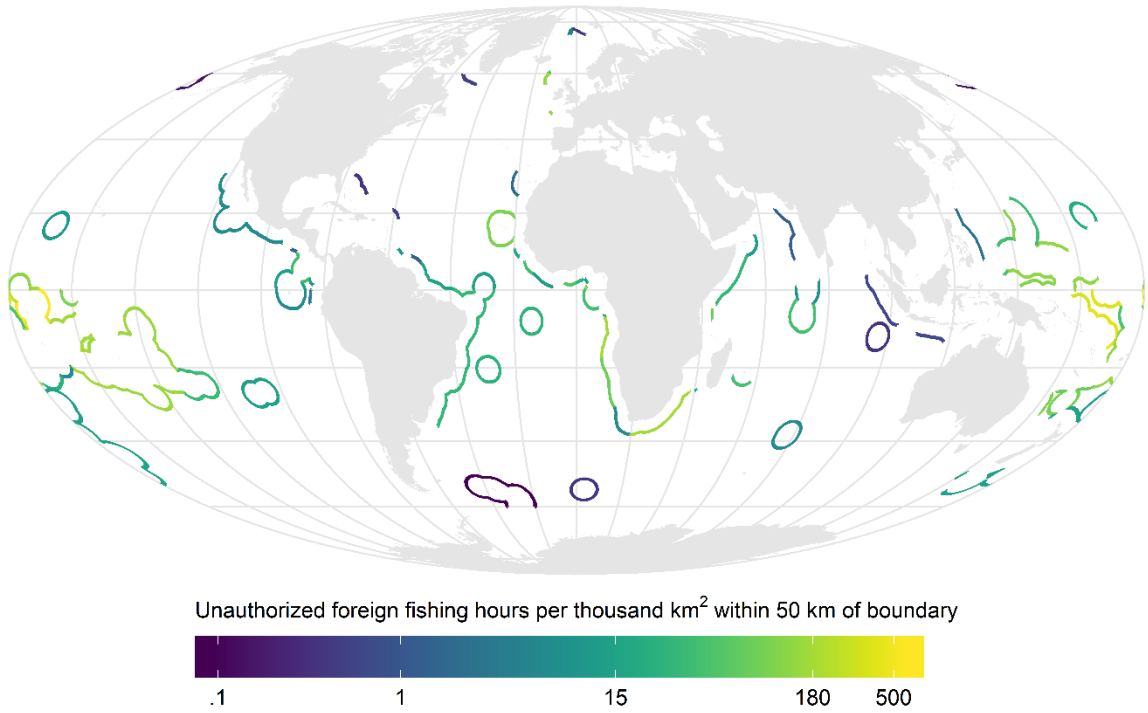

Supplementary Fig. 9. EEZ-sea regions that do not deter unauthorized foreign fishing. These 83 EEZ-sea regions have enough unauthorized foreign fishing within 50 km of their high seas boundary to estimate a deterrence effect (more than 10 hours), but they do not deter unauthorized foreign fishing (unauthorized foreign fishing is higher just inside their EEZ than just outside).

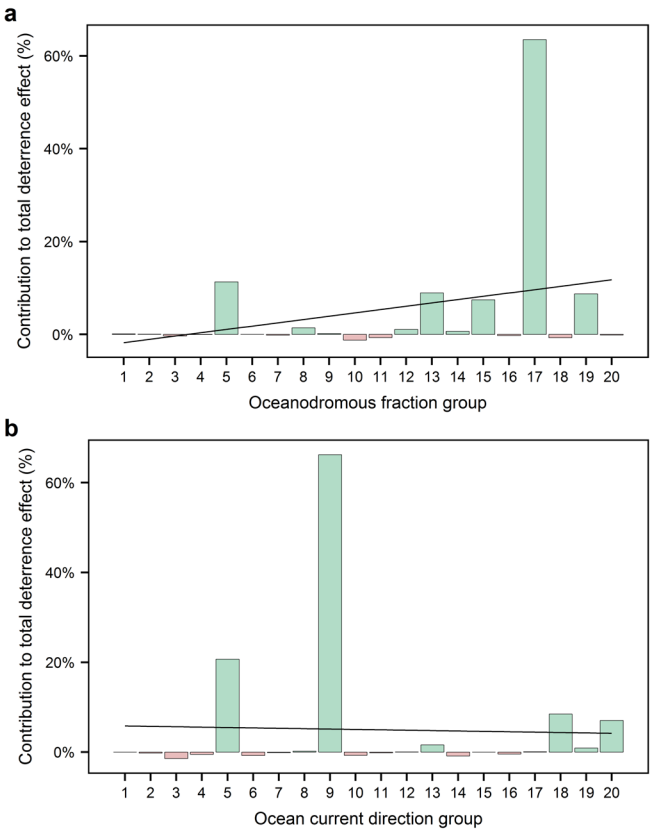

Supplementary Fig. 10. Deterrence effect heterogeneity by fish stock movement patterns. Contribution of each (**a**) oceanodromous fraction group and (**b**) ocean surface current direction group to the total deterrence effect. The creation of these variables is described in Supplementary Methods section 3.5. We estimate a deterrence effect for each quantile group, and divide each group's effect by the sum of all groups' deterrence effects. Quantile groups that contribute a positive percentage (green) deter unauthorized foreign fishing. The black lines are linear trends.

Supplementary Tables

Supplementary Table 1. Effect of EEZs on fishing effort. This table contains numeric estimates corresponding to Fig. 2a-d. The "levels" row displays the estimated effect of EEZs on the untransformed dependent variable. The "logs" row displays the estimated effect of EEZs on the natural log of the dependent variable. Newey-West (NW) standard errors are displayed in parentheses[14]. The optimal NW lag for each regression was chosen using the procedure described in Newey and West[15]. The "percentage" row expresses the effect of EEZs as a percentage difference in fishing just inside EEZs compared to just outside EEZs. This percentage difference uses the estimated effect from the natural log specification and is computed using the formula $100\left(e^{\log \text{effect}} - 1\right)$. All regressions have 98 observations. ***p < 0.01, **p < 0.05, *p < 0.1.

	Fig. 2a	Fig. 2b	Fig. 2c	Fig. 2d	
	Total AIS	VBD	Unauth. For.	Auth. For.	Domestic
	(1)	(2)	(3)	(4)	(5)
Levels	-190,359	-5,496	-195,197	1,927	2,911
	(23,570)***	(608)***	(20,887)***	(686)***	(2,013)
NW lag	2	6	4	4	7
Logs	-1.37	-1.33	-1.66	0.22	0.36
	(0.21)***	(0.10)***	(0.25)***	(0.09)**	(0.10)***
NW lag	3	8	2	4	4
Percentage	-74.6%	-73.5%	-81.0%	24.8%	43.0%

Supplementary Table 2. Gear type composition by vessel type. Each column lists the percentage of AIS fishing hours between 2012 and 2016 from each gear type for a given vessel type. Only fishing within 50 km of an EEZ-high seas boundary is included in this table.

	Unauthorized Foreign	Authorized Foreign	Domestic
Drifting Longlines	46.9%	58.5%	29.9%
Trawlers	22.8%	16.5%	55.1%
Squid Jiggers	26.2%	0.0%	2.0%
Fixed Gear	1.6%	10.8%	4.9%
Purse Seines	2%	13.9%	3.7%
Other	0.4%	0.2%	4.4%
Total Fishing Hours	3,318,382	276,947	561,728

Supplementary Table 3. Mean vessel characteristics by vessel type and gear type. The mean value for a characteristic is weighted by AIS fishing hours within 50 km of an EEZ-high seas boundary between 2012 and 2016. Hours-weighted standard deviations are displayed in brackets.

Geartype	Characteristic	Unauthorized Foreign	Authorized Foreign	Domestic
Drifting Longlines				
	Gross Tonnage	379 [251]	264 [133]	311 [339]
	Length (m)	42.8 [12]	33.2 [10.5]	30.9 [11.5]
	Engine Power (kW)	828 [330]	421 [224]	587 [391]
Trawlers				
	Gross Tonnage	2,287 [1,961]	1,926 [2,341]	1,439 [1,318]
	Length (m)	73.2 [17.7]	61.7 [27.6]	57.7 [19.5]
	Engine Power (kW)	2,967 [1,527]	2,194 [1,822]	2,264 [1,465]
Squid Jiggers				
	Gross Tonnage	925 [313]	NA [NA]	596 [220]
	Length (m)	58.7 [6.7]	NA [NA]	53.5 [4.7]
	Engine Power (kW)	1,321 [356]	NA [NA]	1,246 [243]
Fixed Gear				
	Gross Tonnage	697 [255]	297 [221]	456 [310]
	Length (m)	51.2 [6.4]	32.6 [10.6]	38.4 [13.1]
	Engine Power (kW)	1,097 [274]	556 [402]	693 [299]
Purse Seines				
	Gross Tonnage	1,399 [424]	1,355 [566]	1,402 [447]
	Length (m)	69.3 [8.5]	64.6 [15]	64.9 [11.8]
	Engine Power (kW)	2,728 [655]	2,402 [860]	2,757 [815]
Other				
	Gross Tonnage	574 [438]	265 [163]	740 [550]
	Length (m)	51 [15.3]	37.5 [15.1]	45.3 [13.2]
	Engine Power (kW)	1,354 [565]	694 [438]	1,219 [606]
All Geartypes				
	Gross Tonnage	984 [1,226]	694 [1,185]	1,004 [1,137]
	Length (m)	54.6 [17.5]	42.2 [20.6]	48.3 [20.6]
	Engine Power (kW)	1,490 [1,172]	1,005 [1,194]	1,637 [1,386]

Supplementary Table 4. Deterrence effects excluding observations closest to an EEZ-high seas boundary and using different bandwidths. This table contains numeric estimates corresponding to Supplementary Fig. 4a-e. The "levels" row displays the estimated effect of EEZs on hours of unauthorized foreign fishing effort per million km^2. The "logs" row displays the estimated effect of EEZs on the natural log of hours of unauthorized foreign fishing effort per million km^2. Newey-West (NW) standard errors are displayed in parentheses[14]. The optimal NW lag for each regression was chosen using the procedure described in Newey and West[15]. The "percentage" row expresses the effect of EEZs as a percentage difference in fishing just inside EEZs compared to just outside EEZs. This percentage difference uses the estimated effect from the natural log specification and is computed using the formula $100(e^{\log \text{effect}} - 1)$. The "difference" row is the percentage difference minus the percentage difference in Supplementary Fig. 4a. The "donut hole" row refers to the observations that are excluded from the regression. The "bandwidth" row refers to the data used in the regression. For example, the column (**c**) regression uses unauthorized foreign fishing effort within 100 km of an EEZ-high seas boundary (bandwidth = 100 km), but excludes observations within 10 km of an EEZ-high seas boundary (donut hole = 10 km). See Supplementary Methods section 3.2 for additional details and interpretation of these results. ***p < 0.01, **p < 0.05, *p < 0.1.

	(**a**)	(**b**)	(**c**)	(**d**)	(**e**)
Levels	-201,861 (9,254)***	-203,693 (4,653)***	-195,512 (4,891)***	-217,826 (12,789)***	-189,830 (19,231)***
NW lag	2	2	6	2	5
Logs	-2.11 (0.16)***	-2.29 (0.04)***	-2.20 (0.05)***	-2.29 (0.08)***	-2.14 (0.12)***
NW lag	6	5	6	4	6
Percentage	-87.9%	-89.9%	-88.9%	-89.9%	-88.2%
Difference		-2.0%	-1.1%	-2.0%	-0.3%
Donut hole	0 km	10 km	10 km	25 km	25 km
Bandwidth	50 km	50 km	100 km	50 km	100 km
Observations	98	80	180	50	150

References

1. Kroodsma, D. A. *et al.* Tracking the global footprint of fisheries. *Science* **359,** 904–908 (2018).
2. Elvidge, C. D., Zhizhin, M., Baugh, K. & Hsu, F.-C. Automatic boat identification system for VIIRS low light imaging data. *Remote Sens.* **7,** 3020–3036 (2015).
3. Lam, V. W. Y., Tavakolie, A., Palomares, M. L. D., Pauly, D. & Zeller, D. The Sea Around Us catch database and its spatial expression. in *Global Atlas of Marine Fisheries: A Critical Appraisal of Catches and Ecosystem Impacts* (eds. Pauly, D. & Zeller, D.) 59-67 (Island Press, Washington, 2016).
4. Flanders Marine Institute. Intersect of IHO Sea Areas and Exclusive Economic Zones (version 2). http://www.marineregions.org (2012).
5. Behrenfeld, M. J. & Falkowski, P. G. Photosynthetic rates derived from satellite-based chlorophyll concentration. *Limnol. Oceanogr.* **42,** 1–20 (1997).
6. Amante, C. & Eakins, B. W. ETOPO1 1 Arc-Minute Global Relief Model: Procedures, data sources and analysis. DOI: 10.7289/V5C8276M (2009).
7. OBPG. MODIS Aqua Level 3 SST Thermal IR 8 Day 4km Daytime v2014.0. PO.DAAC, CA, USA. https://doi.org/10.5067/MODSA-8D4D4 (2015).
8. Pauly, D. & Zeller, D (eds.). Sea Around Us Concepts, Design and Data (seaaroundus.org) (2015).
9. Chamberlain, S. Reis, R. S. seaaroundus: Sea Around Us API Wrapper. R package version 1.2.0 (2017).
10. Boettiger, C., Lang, D. T. & Wainwright, P. C. rfishbase: exploring, manipulating and visualizing FishBase data from R. *J Fish Biol.* **81,** 2030-2039 (2012).
11. ESR. OSCAR third degree resolution ocean surface currents. Ver. 1. PO.DAAC, CA, USA. DOI: 10.5067/OSCAR-03D01 (2009).
12. Imbens, G. W. & Lemieux, T. Regression discontinuity designs: A guide to practice. *J. Econometrics* **142,** 615–635 (2008).
13. Rubin, D. B. Estimating causal effects of treatments in randomized and nonrandomized studies. *J. Educ. Psychol.* **66,** 688–701 (1974).
14. Newey, W. K. & West, K. D. A simple, positive semi-definite, heteroskedasticity and autocorrelation consistent covariance matrix. *Econometrica* **55,** 703–708 (1987).
15. Newey, W. K. & West, K. D. Automatic lag selection in covariance matrix estimation. *Rev. Econ. Stud.* **61,** 631–653 (1994).
16. Ferraro, P. J., Sanchirico, J. N. & Smith, M. D. Causal inference in coupled human and natural systems. *Proc. Natl. Acad. Sci. U.S.A.* **116,** 5311-5318 (2019).
17. Barreca, A. I., Guldi, M., Lindo, J. M., & Waddell, G. R. Saving Babies? Revisiting the effect of very low birth weight classification. *Q. J. Econ.* **126,** 2117–2123 (2011).
18. Hollick, A. L. The origins of 200-mile offshore zones. *Am. J. Int. Law* **71,** 494–500 (1977).
19. Hannesson, R. Exclusive Economic Zone. in *Encyclopedia of Energy, Natural Resource, and Environmental Economics* (ed. Shogren, J. F.) 150-153 (Elselvier, 2013).